Copper-Intercalated TiS_2: Electrode Materials for Rechargeable Batteries as Future Power Resources

Ali H. Reshak*

Institute of Physical Biology, South Bohemia University, Institute of System Biology and Ecology, Academy of Sciences, Nove Hrady 37333, Czech Republic

Received: November 21, 2008; Revised Manuscript Received: December 18, 2008

We report results of first-principles total-energy calculations of structural and optical properties of the TiS_2 single crystals intercalated with copper. Calculations have been performed using an all-electron, full potential, linearized, augmented, plane-wave method based on density functional theory using generalized gradient approximation for the exchange correlation energy functional. To complete the fundamental characteristics of these compounds, we have calculated and analyzed their linear optical susceptibilities. We demonstrate the efficiency of using a full potential on the band structure, density of states, and the optical properties. We compare our results of the intercalated Cu in different sites and concentrations with the host TiS_2 compound to ascertain the effect of Cu intercalation on the electronic and optical properties. Our calculations have shown that the electronic and optical properties are influenced significantly by the location and concentration of the Cu intercalate in the host compound. The Cu-s and Cu-p bands are very broad and do not contribute much to the density of states. The density of states and the electron charge density show that all Ti−Ti and S−S bonds are basically of ionic character and that Ti−S bonds are of covalent character. No covalent electrons are found between Cu and S atoms; that is, no covalent bond exists between the Cu and S atoms. The Cu atoms are ionic in the intercalated compounds.

I. Introduction:

Copper batteries are among the best battery systems in terms of energy density. This makes them very attractive for hybrid automobiles and portable electronics. Layered Cu metal chalcognides described by the formula $CuMX_2$ have been the focus of much attention as Cu insertion cathodes for use with a Cu-intercalated carbon anode. These materials are of great interest because they act as host lattices by reacting with a variety of guest atoms or molecules to yield intercalation compounds, in which the guest is inserted between the host single-crystal layers.[1] In layered MS_2 materials, atoms within a layer are bound by strong ionic-covalent forces, while the individual layers are held together by weak van der Waals (vdW) interactions. The weak interlayer vdW interactions allow doped atoms or molecules to be introduced between the layers through intercalation.[2]

High-energy-density researchable batteries are needed for development of long-range electric vehicles to improve the air quality in congested cities and as acceptable good alternative power sources for the future. For versatile uses, the availability of an ambient temperature researchable battery is then an essential goal. The most promising approach to achieve this goal so far has been the effort directed toward the production of the third nonaqueous system, Cu batteries; that is, batteries based on Cu metal or a Cu ion source anode, a Cu ion conducting electroyte, and a Cu ion accepting cathode material. The latter is generally an open-structured compound capable of accepting and releasing Cu ions into and out of its crystal lattice. Typical examples are transition metal dichalcogenides.[3] The group IVB, VB, and VIB transition metal disulfides have a rather unusual two-dimensional layer structure which can intercalate atoms rapidly and reversibly.[4,5]

As far as the intercalation process is concerned, lamellar transition metal disulfides remain the best example, even if they are no longer considered as attractive materials in rechargeable battery design. Among these sulfides; TiS_2 is especially interesting because it is one of the very few examples of a host structure that is deeply modified by Cu intercalation, resulting in dramatic loss of crystallinity.

The titanium dichalcogenide compound TiS_2 has been studied extensively because of its interesting structural and electronic properties. TiS_2 shows a great potential for a variety of technological applications.[6] This compound consists primarily of a hexagonal sheet of cationic Ti atoms sandwiched between two similar sheets of chalcogenic (S) atoms, forming the principal X−Ti−X sandwich. The sheets are coupled by relatively weak van der Waals forces, whereas the atoms within the sheet are coupled by strong covalent ionic bonds. The TiS_2 compound has highly anisotropic physical properties, so much so that they can be regarded as two-dimensional solids. As a result of this, the TiS_2 can be intercalated with foreign atoms and molecules, leading to significant changes in their electronic properties, in particular, in the energy dispersion, and making them technologically competitive.

There exist a number of band structure calculations for the TiS_2 compound.[7−19] Measurement of the polarized X-ray absorption near-edge spectra,[20−22] thermoreflectance,[23] and infrared spectra[24] of these compounds in charged density wave (CDW) states has further contributed to the interest in these compounds. The optical properties of the TiX_2 compounds have been measured by several researchers.[8,9,23,25−29] As a natural extension of our previous work[30−34] of 2H-MoS_2, 1T-/2H-TaS_2 /Se_2, 1T-TiX_2 (X = S, Se, Te), 1T-TiS_2 intercalated with lithium, and 2H-WSe_2 intercalated with Cu. We thought it would also be interesting to perform calculations of TiS_2 intercalated with

* Phone: +420 777729583. Fax: +420-386 361231. E-mail: address: maalidph@yahoo.co.uk.

10.1021/jp810242w CCC: $40.75
Published on Web 01/30/2009

different sites and concentrations of Cu and to study the effect of intercalated Cu on the structural and optical properties.

Even though there are experimental measurements[35−40] which throw light on the electronic properties of Cu-intercalated TiS_2, to the best of our knowledge, the theoretical calculations of the structural and optical properties of these compounds are nonexistent. It would be useful to do natural extension and more precise calculations based on full potential methods. Such calculations are reported in this paper. With this in mind, we report calculations of the electronic and optical properties of TiS_2 and its intercalated compounds using the full potential linearized augmented plane wave (FPLAPW) method and compare them with available experimental data. Our calculations will demonstrate the effect of using a full potential on the band structure, density of states (DOS), and the optical properties. In particular, our calculations could throw light on the effect of intercalation on band structure, DOS, and optical properties. We compare our results with TiS_2 (our previous work)[32,33] to ascertain the effect of Cu intercalation (different sites and concentrations) on the electronic and optical properties.

The recent explosion in the portable electronics market has provoked a need for more environmentally friendly batteries, away from such toxic heavy-metal based concepts as Pb-acid, Hg, and NiCd. This has meant that research effort in electrode and electrolyte materials for state-of-the-art rechargeable batteries has greatly intensified. We are studying the structural and other properties of these innovative materials, as these may well prove the limiting factor in exploiting otherwise ideal battery materials.

In Section II, we give details of our calculations. The band structure and density of states are presented and discussed in Section III.a. The frequency-dependent dielectric function is given in Section III.b, and Section IV summarizes our conclusions.

II. Structural Aspects and Computational Details

The host compound, TiS_2, is crystallized in hexagonal structure with space group $P\bar{3}m1$, no. 164. For the intercalated compounds, the structural calculations were performed with Cu atoms occupying the octahedral and tetrahedral sites (see Figure 1). Here, we used two concentrations of Cu ($x = 0.384$ and 0.2106) in the octahedral sites and one concentration of Cu ($x = 0.36$) for the tetrahedral sites. These are $Cu_{0.384}TiS_2$, $Cu_{0.2106}TiS_2$, and $Cu_{0.36}TiS_2$, respectively, which are crystallized in the hexagonal structures (space group $P\bar{3}m1$, no. 164). The other intercalated compound is $Cu_{0.652}Ti_2S_4$, with a Cu concentration of 0.652, crystallized in a face center cubic structure (space group $Fd\bar{3}m$, no. 227). For $Cu_{0.384}TiS_2$ and $Cu_{0.2106}TiS_2$, we intercalated the Cu atom at the (0, 0, 0.5) position, and for $Cu_{0.36}TiS_2$, at the (0, 0, 0.526) position. The Ti atom is located at 1c (origin), and the two S atoms at the 2d (1/3, 2/3, **z**) and (2/3, 1/3, −**z**) positions; for $Cu_{0.652}Ti_2S_4$, the Cu atom was intercalated at the (0.125, 0.125, 0.125) position, the Ti atom is located at the (0.5, 0.5, 0.5) position, and the S atom at the (0.254, 0.254, 0.254) position. We have performed calculations at ambient pressure using the experimental lattice constants **a** and **c** for the host and the intercalated compounds. The distortion from the octahedral configuration is expressed by the quantity **z**, the distance between Ti and the chalcogen plane in units of the lattice constant, **c**, perpendicular to the layers. For the value of **c** in the case of TiS_2 and in-layer lattice constant **a**, it should be 0.2404 in the ideal octahedral case, but actually, it is 0.25.[41] We have performed calculations of the electronic band energy structure and the optical susceptibilities applying the FPLAPW method as incorporated in WIEN2K code.[42] This is an implementation of density functional theory (DFT)[43] with different possible approximations for the exchange correlation potentials. The exchange correlation potential was calculated using the generalized gradient approximation PBE.[44] To achieve desirable energy eigenvalue convergence, the wave functions in the interstitial regions were expanded in plane waves with a cutoff K_{max} of $9/R_{MT}$, where R_{MT} denotes the smallest atomic sphere radius and K_{max} gives the magnitude of the largest K vector in the plane wave expansion. The valence wave functions inside the spheres were expanded up to $l_{max} = 10$, whereas the charge density was Fourier-expanded up to $G_{max} = 14$ (a.u.)$^{-1}$. Self-consistency was achieved using 350 k-points in the irreducible Brillouin zone (IBZ). The IBZ integration was carried out numerically using the tetrahedron method.[45,46] The structural and optical properties were calculated using 500 k-points in IBZ. The calculations were assumed to be converged when the total energy of the system was stabilized within 10^{-5} Ry.

III. Results and Discussion

a. Band Structure and Density of States. For the sake of consistency and to compare with the results for $Cu_{0.384}TiS_2$, $Cu_{0.2106}TiS_2$, $Cu_{0.36}TiS_2$, and $Cu_{0.652}Ti_2S_4$, for different sites and concentrations of Cu atoms, we have reproduced the results of our earlier calculation for TiS_2.[32] The band structure and the total density of states along with the Ti-s/p/d, S-s/p and Cu-s/p/d partial DOS for the host compound TiS_2 and the intercalated compounds are shown in Figures 2 and 3. The band structure and the DOS can be divided into four distinct spectral groups/structures for the host, and three distinct spectral groups/structures for the intercalated compounds. We note that the third and fourth groups/structures of TiS_2 are merged when TiS_2 is intercalated with Cu.

From the band structure and DOS of the host TiS_2, we note that the lowest bands in the energy range between −12.0 and −14.0 eV originated mainly from S-s states. The bands from −5.0 to 2.0 eV (second group) and the bands around 3.5 eV (third group) are mainly S-p states and Ti-d states. The last group is composed of S-p and Ti-s/p/d states.

After Cu is intercalated in the host compound, the band structure and DOS of the intercalated compounds show that all the bands/groups are shifted toward lower energies, resulting in more conduction bands' being pushed toward the valence bands. As a consequence of this intercalation, more bands cut the Fermi energy (E_F), causing the metallic nature of these compounds to increase.

In all intercalated compounds, the lowest group is mainly from S-s states. The second and third groups are composed of Ti-d, Cu-d, S-p with very small contribution from Cu-s/p, and Ti-s/p. We note that increasing the concentration of Cu in the octahedral sites will not cause any significant effect, although as a result of changing Cu from the octahedral to the tetrahedral sites, there is a significant shift of the whole structures toward lower energies by around 3.0 eV, with a reduction in the peak heights and a separations among the second, third, and fourth groups by a gaps of about 0.5 eV. Moving from hexagonal structures of Cu_xTiS_2 to the cubic structure $Cu_{0.652}Ti_2S_4$, we notice a considerable increase in the peak heights, also causing separation of the structures into four distinguishable regions.

The bandwidth to which Ti-d and S-s states make a large contribution is about 10 eV. Therefore, we can conclude that Ti-d and S-s electrons should be treated not as localized electrons but as itinerant electrons.

We found that Ti-s/p/d, Cu-s/p/d, and S-p states controlled the overlapping around E_F. The DOS at Fermi energy (E_F) is

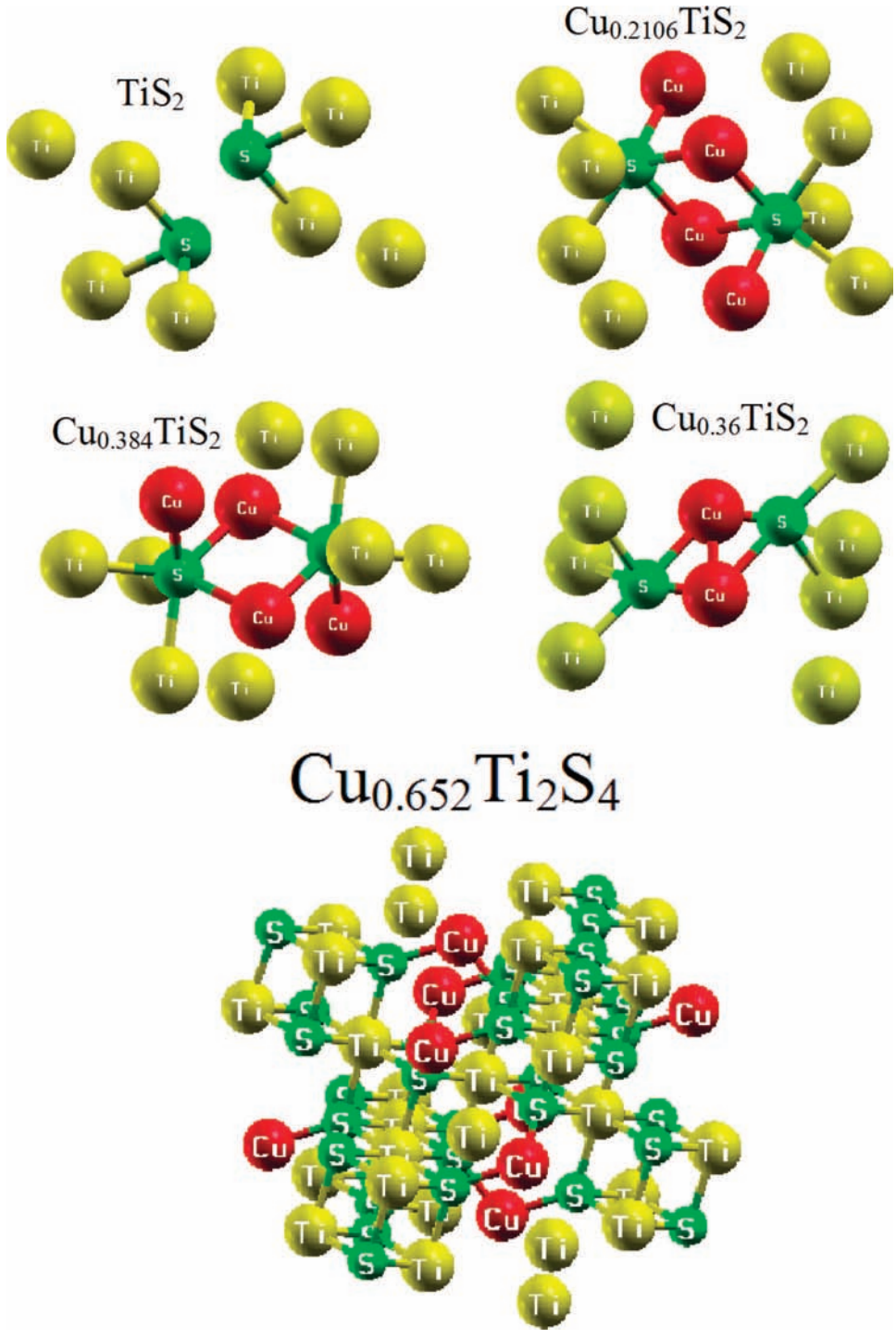

Figure 1. The crystal structure of TiS_2 and its intercalated compounds $Cu_{0.384}TiS_2$, $Cu_{0.2106}TiS_2$, $Cu_{0.36}TiS_2$, and $Cu_{0.652}Ti_2S_4$.

determined by the overlap between the valence and conduction bands. This overlap is strong enough to indicate metallic origin with different values of DOS at E_F, $N(E_F)$ (Table 1). The electronic specific heat coefficient (γ), which is a function of density of states, can be calculated using the expression,

$$\gamma = \frac{1}{3}\pi^2 N(E_F) k_B{}^2 \qquad (1)$$

Here, $N(E_F)$, is the density of states at Fermi energy, and k_B is the Boltzmann constant. The calculated density of states at Fermi energy$N(E_F)$, enables us to calculate the bare electronic specific heat coefficient (Table 1).

From the partial DOS, we are able to identify the angular momentum character of the various structures. For the host compound, the DOS at Fermi energy is determined by the overlap between the S-p states (valence band) and Ti-d states (conduction band). This overlap is small for TiS_2, indicating a semimetallic origin with a DOS at E_F, $N(E_F)$ of 0.35 (state/eV unit cell), in agreement with the value of 0.39 (state/eV unit cell) obtained by Takahira et al.[47] using the self-consistent APW method and 0.37 (states/eV unit cell) obtained by Kim et al.[48] using the discrete-variational Xα cluster method, whereas when TiS_2 is intercalated with Cu, we found the DOS at E_F, $N(E_F)$, increased, depending on the location and the concentration of Cu in the host compound (Table 1). That is attributed to the fact that intercalated TiS_2 with Cu leads to pushing both Ti-d (CB) and S-p (VB) forward the E_F to overlap very strongly

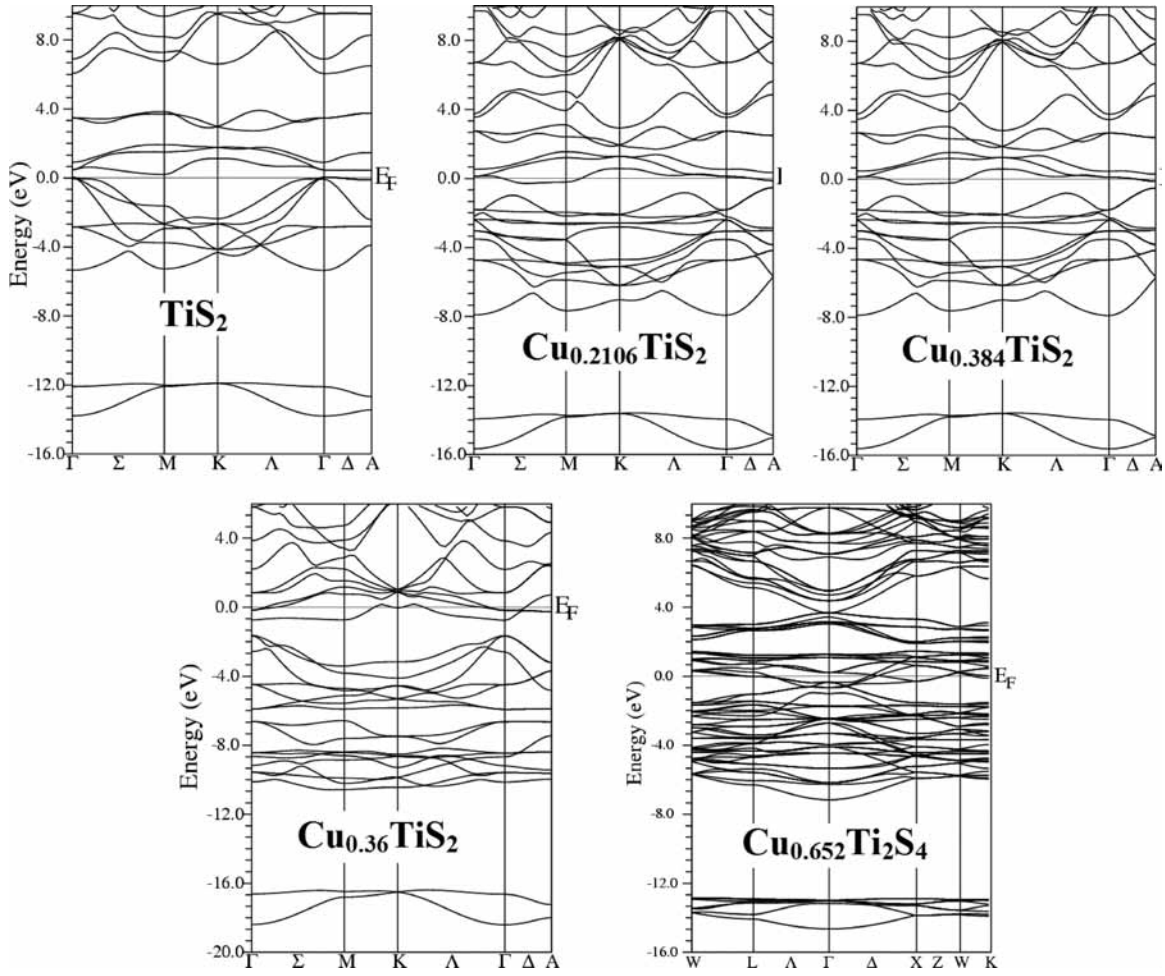

Figure 2. Calculated band structure for the host material TiS_2 and its intercalated compounds $Cu_{0.384}TiS_2$, $Cu_{0.2106}TiS_2$, $Cu_{0.36}TiS_2$, and $Cu_{0.652}Ti_2S_4$.

around E_F. Thereby, intercalated Cu drastically changes the band structure, resulting in more bands cutting E_F, making the intercalated compounds very good metallic compounds. The intercalation compounds are of great interest because of their low dimensional properties[49,50] and application as a high-density energy battery.[51]

From the band structure and PDOS of TiS_2, one can see that there exists a strong hybridization between S-p states and Ti-d states below E_F. This hybridization becomes week in the intercalated compounds. In all intercalated compounds, Cu-s strongly hybridizes with Cu-p below and above E_F. The Cu-intercalated compounds have a very small contribution from the Cu-s and Cu-p states. Cu-s and Cu-p bands are very broad energetically, extending from −16 to 10 eV. The number of electrons inside the Cu muffin-tin sphere in the Cu-intercalated compound is the same as in the pure Cu atom, indicating a very weak hybridization with the Ti and S states.

Now we elucidate the feature of chemical bonding from the nature of total DOS and angular momentum projected DOS (partial DOS). We observe that for the host material TiS_2, the DOS, ranging from −8.0 eV to E_F, is larger for Ti-d states (2.0 electrons/eV), S-p states (1.8 electrons/eV), Ti-p (0.08 electrons/eV), and Ti-s (0.05 electrons/eV) by comparing the total DOS with the angular momentum projected DOS of Ti-d, S-p, Ti-p, and Ti-s, states as shown in Figure 3. These results show that some electrons from Ti-d, S-p, Ti-s, and Ti-p states transfer into VBs and take part in weak covalence interactions between Ti−Ti and S−S atoms and the substantial covalence interactions between Ti and S atoms. All the Ti−Ti and S−S bonds are basically of ionic character, and Ti−S bonds are of covalent character. Accordingly, we can also say that the covalent strength of Ti−S bonds is stronger than that of Ti−Ti or S−S bonds. For the Cu-intecalated compounds, the DOS, at the same range as for the host compound, is larger for Cu-d states (2.5 − 4.0 electrons/eV), Ti-d (1.0 − 1.5 electrons/eV), and S-p states (0.5 −2.2 electrons/eV). By comparing the total DOS with the angular momentum projected DOS of Cu-d, Ti-d, and S-p, states (Figure 3), we found that some electrons from Cu-d, Ti-d, and S-p, states transfer into VBs and take part in weak covalence interactions between Ti−Ti and S−S atoms and the substantial covalence interactions between Ti and S atoms. We also found that similar to the host compound, all the Ti−Ti and S−S bonds are basically of ionic character, and Ti−S bonds are of covalent character. No covalent electrons are found between Cu and S atoms; that is, no covalent bond exists between the Cu and S atoms. The Cu atoms are ionic in these compounds.

Turning now to the bonding properties, to visualize the nature of the bond character and to explain the charge transfer and bonding properties of $Cu_{0.36}TiS_2$, $Cu_{0.2106}TiS_2$, $Cu_{0.384}TiS_2$, $Cu_{0.652}Ti_2S_4$, and TiS_2, we calculated the total valence charge density. We show in Figure 4 the total valence charge densities in the (110) plane for each material. For TiS_2, it seems that a strong covalent bond exists between the Ti and S atoms (Figure 4a). The Ti−Ti and S−S bonds are found to be weaker than the Ti−S bond (Figure 4a), which shows that a covalent bond exists between Ti and S atoms. The electron density distribution

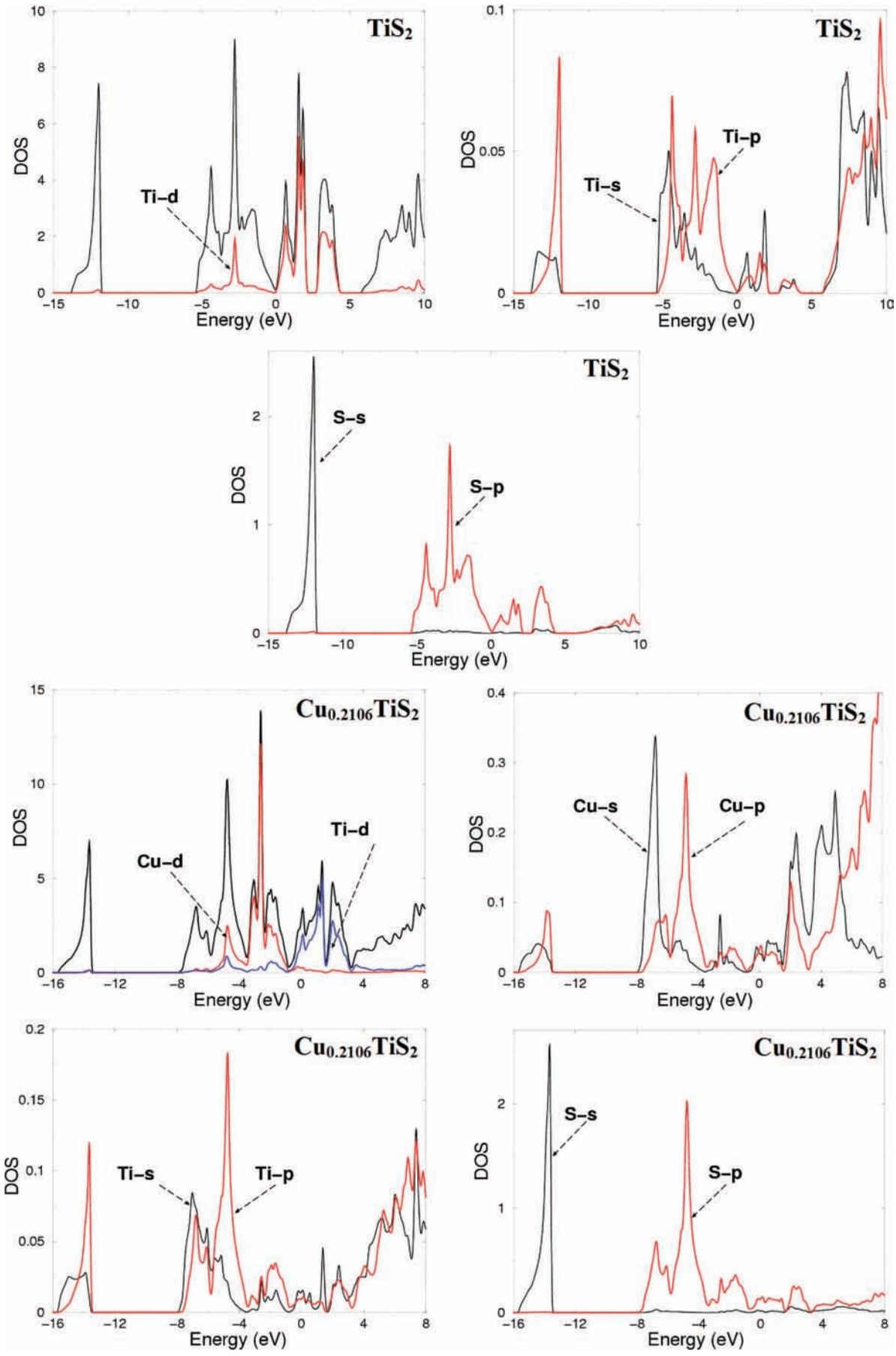

Figure 3. Part 1 of 3.

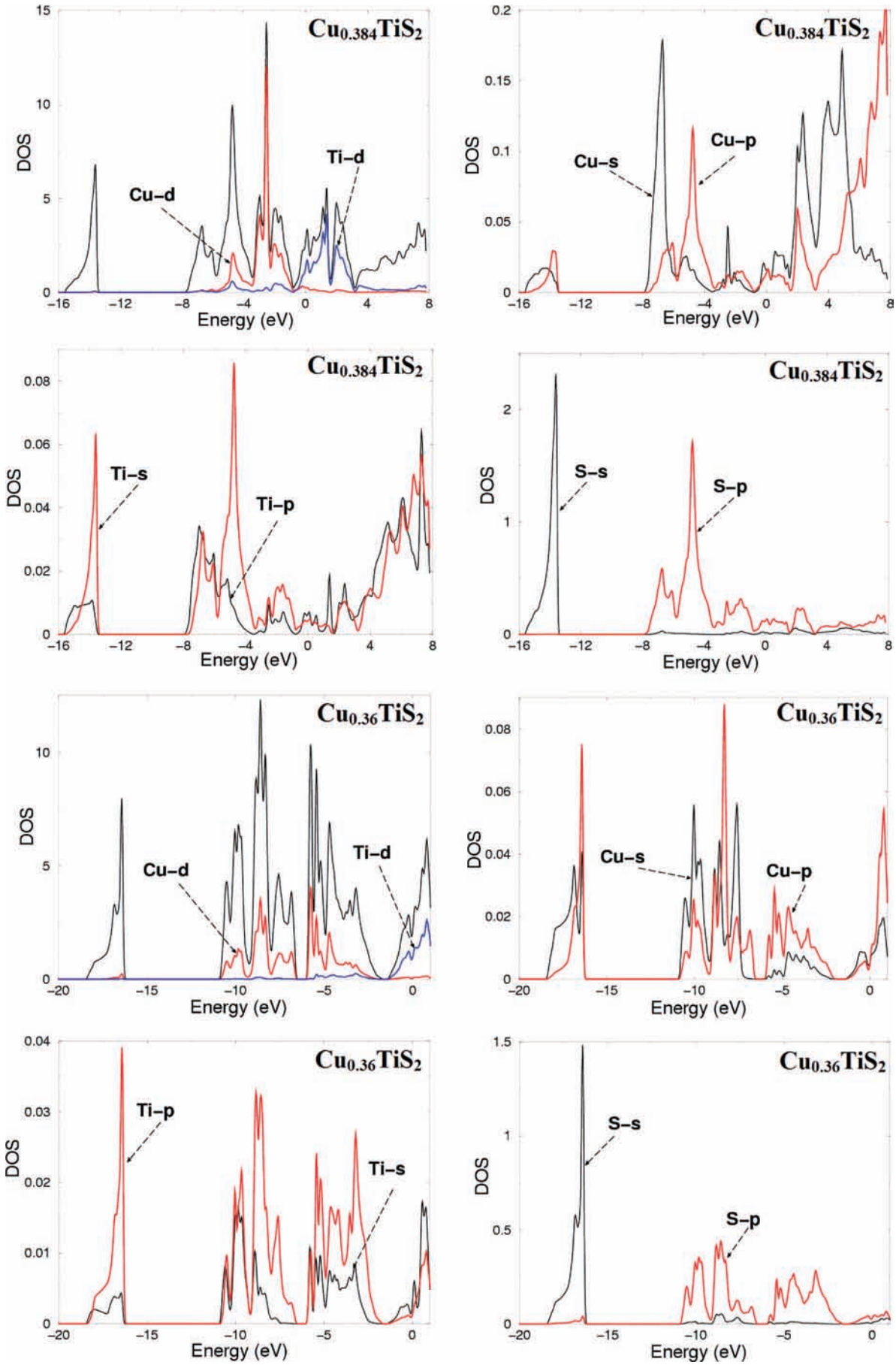

Figure 3. Part 2 of 3.

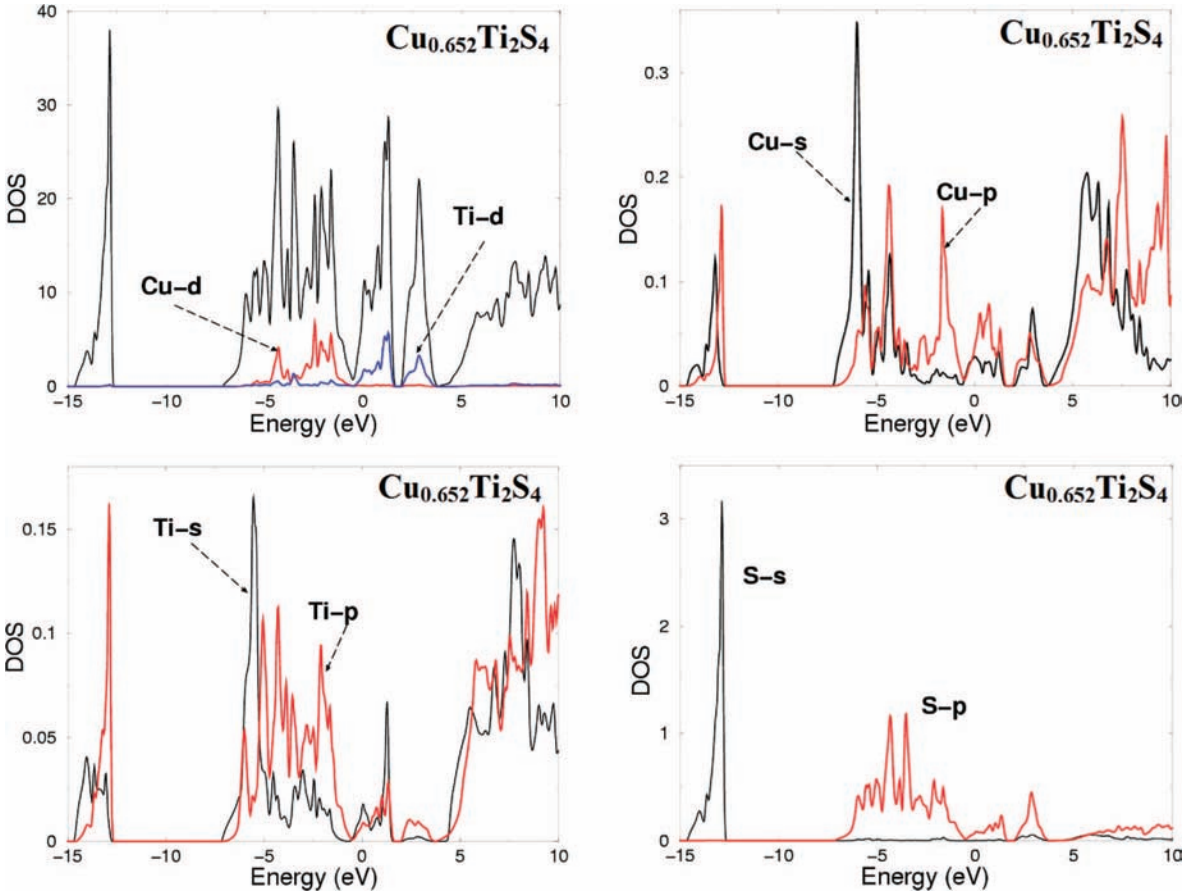

Figure 3. Part 3 of 3. Total density of states (states/eV unit cell) along with the partial density of states for the host material, TiS_2, and its intercalated compounds $Cu_{0.384}TiS_2$, $Cu_{0.2106}TiS_2$, $Cu_{0.36}TiS_2$, and $Cu_{0.652}Ti_2S_4$.

of the intercalated Cu atom was compared with that of TiS_2, and it shows that a covalent bond exists between Ti and S atoms. On the other hand, no extra electrons are found between the Cu and S atoms, which means that the intercalated Cu atoms are located as ionic atoms in the layer of the van der Waals gap and no covalent bond exists between Cu and S.

b. Optical Properties. The optical properties of solids are a major topic, both in basic research and for industrial applications. Although for the former, the origin and nature of different excitation processes is of fundamental interest, the latter can make use of them in many optoelectronic devices. These wide interests require experiment and theory. The calculations of the frequency-dependent dielectric function involve the energy eigenvalues and electron wave functions. These are natural outputs of band structure calculations. $Cu_{0.652}Ti_2S_4$ has a face-centered cubic structure with space group $Fd3m$. For calculating the optical properties of cubic structural material, we need only one dielectric tensor component to completely characterize the linear optical properties. This component is $\varepsilon_2(\omega)$, the imaginary part of the frequency dependent dielectric function is given by[52]

$$\varepsilon_2(\omega) = \frac{8}{3\pi\omega^2}\sum_{nn'}\int_{BZ}\left|P_{nn'}(k)\right|^2\frac{\mathrm{d}S_k}{\nabla\omega_{nn'}(k)} \qquad (2)$$

where $P_{nn'}(k)$ is the dipolar matrix elements between initial $|nk\rangle$ and final $|n'k\rangle$ states with their eigenvalues $E_n(k)$ and $E_{n'}(k)$, respectively.

The other compounds, TiS_2, $Cu_{0.384}TiS_2$, $Cu_{0.2106}TiS_2$, and $Cu_{0.36}TiS_2$, having hexagonal symmetry, the experiments are performed with electric vector $\vec{E}$ parallel or perpendicular to the c axis. The corresponding dielectric functions are $\varepsilon^{\parallel}(\omega)$ and $\varepsilon^{\perp}(\omega)$. We have performed calculations of the imaginary part of the interband frequency-dependent dielectric function using the expressions[53]

$$\varepsilon_2^{\mathrm{II}}(\omega) = \frac{12}{m\omega^2}\int_{BZ}\sum_{nn'}\frac{\left|P^Z_{nn'}(k)\right|^2\mathrm{d}S_k}{\nabla\omega_{nn'}(k)} \qquad (3)$$

$$\varepsilon_2^{\perp}(\omega) = \frac{6}{m\omega^2}\int_{BZ}\sum_{nn'}\frac{\left[\left|P^X_{nn'}(k)\right|^2+\left|P^Y_{nn'}(k)\right|^2\right]\mathrm{d}S_k}{\nabla\omega_{nn'}(k)} \qquad (4)$$

The above expressions are written in atomic units with $e^2 = 1/m = 2$ and $\hbar = 1$. Where $\hbar\omega$ is the photon energy. $P^X_{nn'}(k)$ and $P^Z_{nn'}(k)$ are the X and Z components of the dipolar matrix elements between initial $|nk\rangle$ and final $|n'k\rangle$ states with their eigenvalues $E_n(k)$ and $E_{n'}(k)$, respectively. $\omega_{nn'}(k)$ is the interband energy difference

$$\omega_{nn'}(k) = E_n(k)\ E_{n'}(k) \qquad (5)$$

and S_k is a constant energy surface, $S_k = \{k; \omega_{nn'}(k) = \omega\}$. The integral is over the first Brillouin zone.

The optical properties can be described by the mean of the transverse dielectric function, $\varepsilon(\omega)$. For the metallic and semimetallic materials, there are two contributions to $\varepsilon(\omega)$; namely, intraband and interband transitions. Because the investigated compounds are metallic, we must include the Drude term (intraband transitions).[54]

$$\varepsilon_2^{\perp}(\omega) = \varepsilon^{\perp}_{2\mathrm{inter}}(\omega) + \varepsilon^{\perp}_{2\mathrm{intra}}(\omega) \qquad (6)$$

where

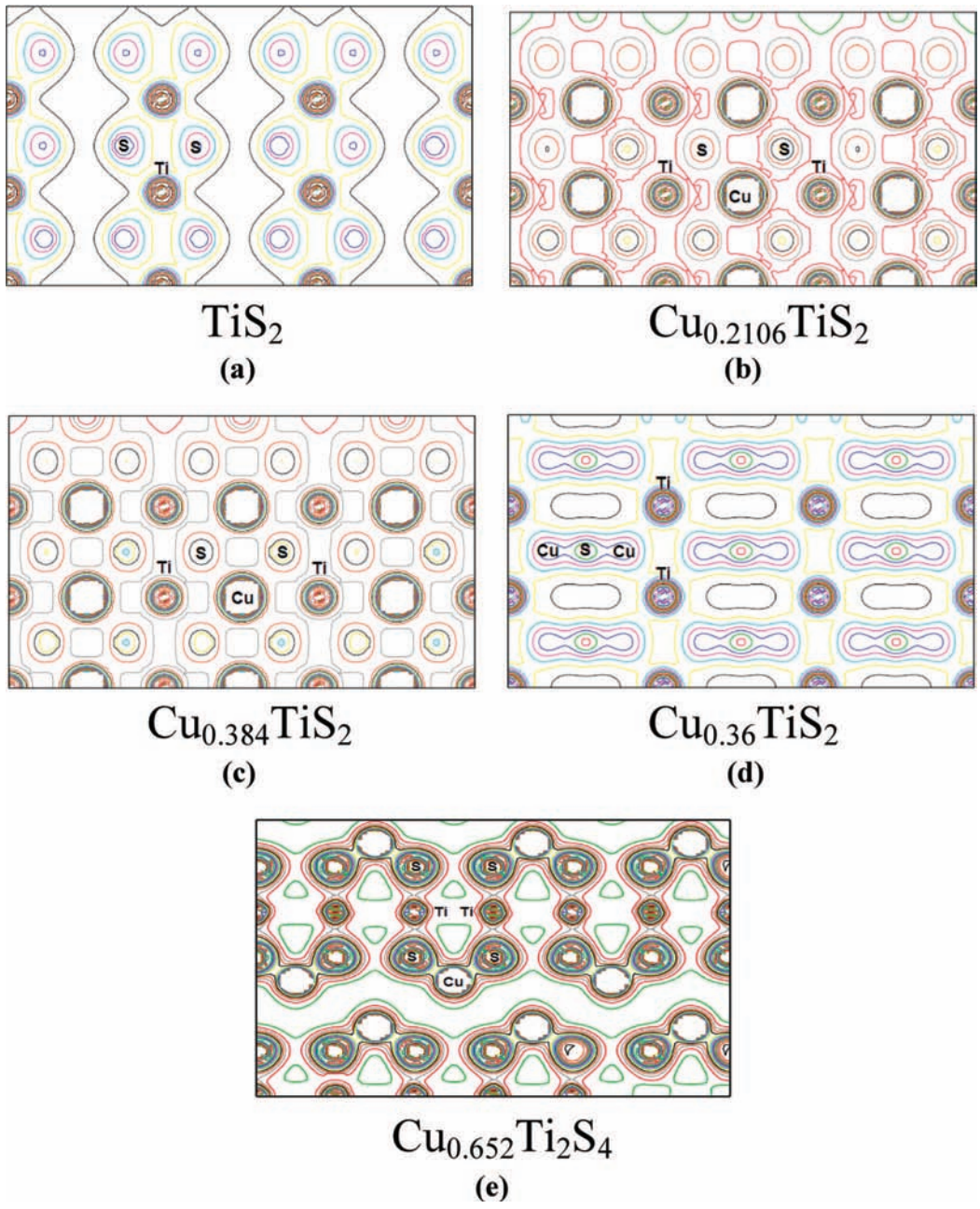

Figure 4. Total valence charge densities in the (110) plane for (a) TiS_2, (b) $Cu_{0.2106}TiS_2$, (c) $Cu_{0.384}TiS_2$, (d) $Cu_{0.36}TiS_2$, and (e) $Cu_{0.652}Ti_2S_4$.

TABLE 1: The Density of States at Fermi Energy $N(E_F)$ States/Ry Cell, the Bare Electronic Specific Heat Coefficient γ (mJ/mol K^2), and the Plasma Frequencies for the Host Material TiS_2 and Its Intercalated Compounds $Cu_{0.384}TiS_2$, $Cu_{0.2106}TiS_2$, $Cu_{0.36}TiS_2$, and $Cu_{0.652}Ti_2S_4$

	TiS_2	$Cu_{0.2106}TiS_2$	$Cu_{0.384}TiS_2$	$Cu_{0.36}TiS_2$	$Cu_{0.652}Ti_2S_4$
$N(E_F)$ states/Ry cell	4.76	36.72	36.72	28.56	136
γ (mJ/mol K^2)	0.82	6.37	6.37	4.95	23.59
$\omega_P^{\parallel}$ (ω)	0.22	2.38	2.37	2.09	2.73
$\omega_P^{\perp}$ (ω)	0.28	4.59	4.55	3.36	2.73

$$\varepsilon_{2\text{int}ra}^{\perp}(\omega) = \frac{\omega_P^{\perp}\tau}{\omega(1+\omega^2\tau^2)} \tag{7}$$

where ω_P is the anisotropic plasma frequency[57] and τ is the mean free time between collisions.

$$\omega_P^{\perp 2} = \frac{8\pi}{3}\sum_{kn} \vartheta_{kn}^{\perp 2}\,\delta(\varepsilon_{kn}) \tag{8}$$

where ε_{kn} is $E_n(k) - E_F$, and $\vartheta_{kn}^{\perp}$ is the electron velocity (in basal plane) squared. Similarly, expressions for the parallel component can be written. In Table 1, we have listed the values of the plasma frequency for the host and Cu-intercalate compounds.

Figure 5, shows the calculated $\varepsilon_2^{\parallel}(\omega)$, $\varepsilon_2^{\perp}(\omega)$, and $\varepsilon_2(\omega)$ spectra for host and Cu-intercalated compounds. We have performed the calculations of $\varepsilon_2^{\parallel}(\omega)$, $\varepsilon_2^{\perp}(\omega)$, and $\varepsilon_2(\omega)$ with and without inclusion of the Drude term. The effect of the Drude term is significant for energies <1 eV. The sharp rise at low energies

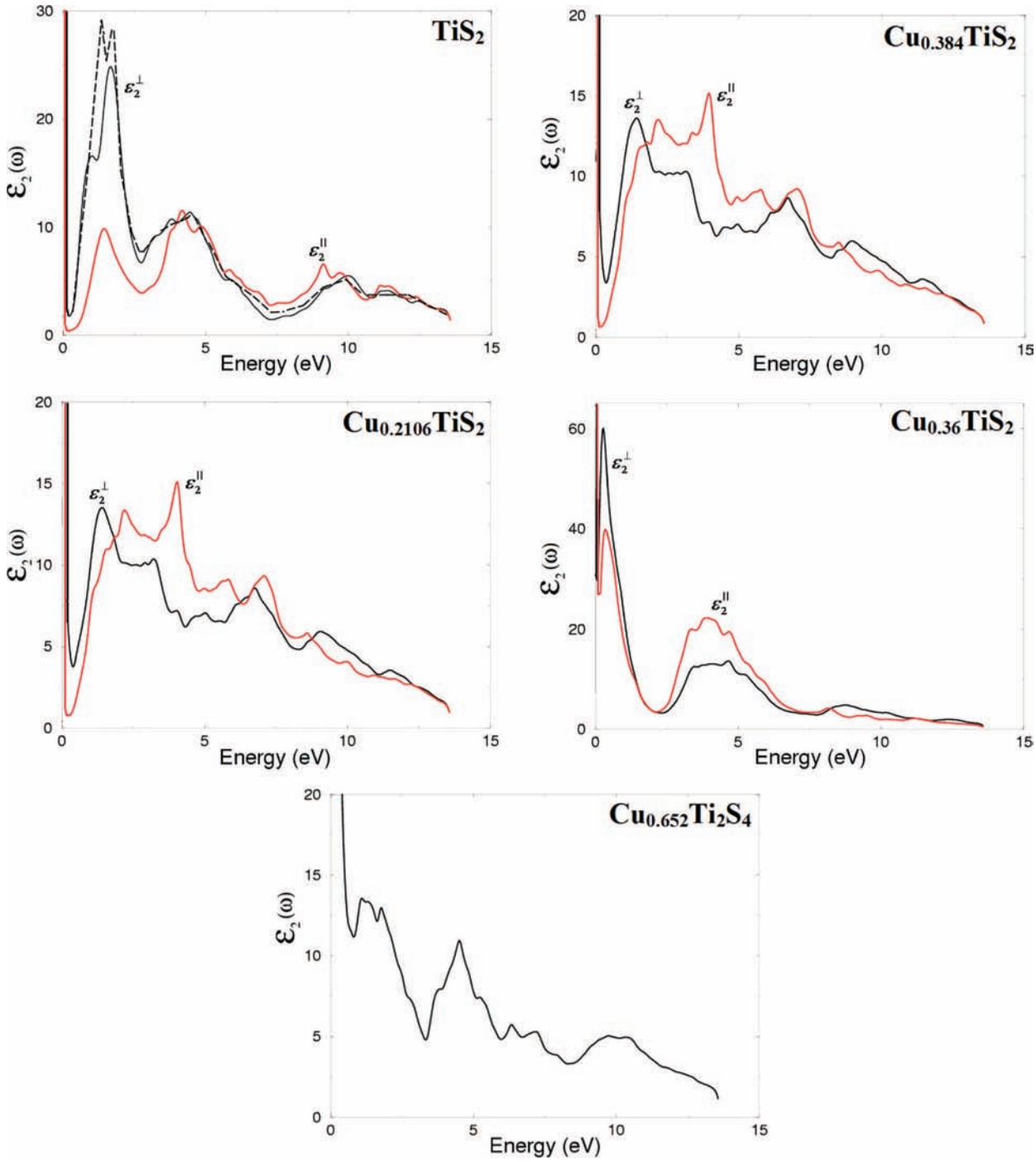

Figure 5. Calculated $\varepsilon_2(\omega)$, $\varepsilon_2^{\perp}$ (ω) (dark curve) and $\varepsilon_2^{\text{II}}(\omega)$ (light curve) for the host material TiS_2 and its intercalated compounds $Cu_{0.384}TiS_2$, $Cu_{0.2106}TiS_2$, $Cu_{0.36}TiS_2$, and $Cu_{0.652}Ti_2S_4$. In comparison with the available experimental data of $\vec{E} \perp c$[26] (dashed curve), for the host material TiS_2.

is due to the Drude term. We note that there is a considerable anisotropy between $\varepsilon_2^{\text{II}}(\omega)$ and $\varepsilon_2^{\perp}(\omega)$. Our calculations show that intercalated Cu causes a shift of all the structure toward lower energies, with significant reduction in the height of the peaks, except that in the compound in which Cu occupies the tetrahedral sites, the height of the peaks is significantly increased in comparison with the structures in TiS_2. The shifting of the structures is consistent with our calculated band structure and corresponding density of states. In contrast to the host compound, $\varepsilon_2^{\text{II}}(\omega)$ dominates in the low energy range for the intercalated compounds. Thereafter, both polarizations contribute in both the host and Cu-intercalated compounds. We compare our calculated dielectric constant with the available experimental data;[26] for $\vec{E}$ c, good agreement was found.

Generally, the spectral peaks in the optical response are determined by the electric dipole transitions between the occupied and unoccupied bands. These peaks can be identified from the band structure. To identify these peaks, we need to look at the optical transition dipole matrix elements. We analyzed the optical spectra of $\varepsilon_2^{\text{II}}(\omega)$, $\varepsilon_2^{\perp}(\omega)$, and $\varepsilon_2(\omega)$. We have found that the transitions that are responsible for the structures below 5 eV in $\varepsilon_2^{\text{II}}(\omega)$, $\varepsilon_2^{\perp}(\omega)$, and $\varepsilon_2(\omega)$ are dominated by transitions from bands just below Fermi energy (E_F) to bands just above it, whereas the transitions that are responsible for

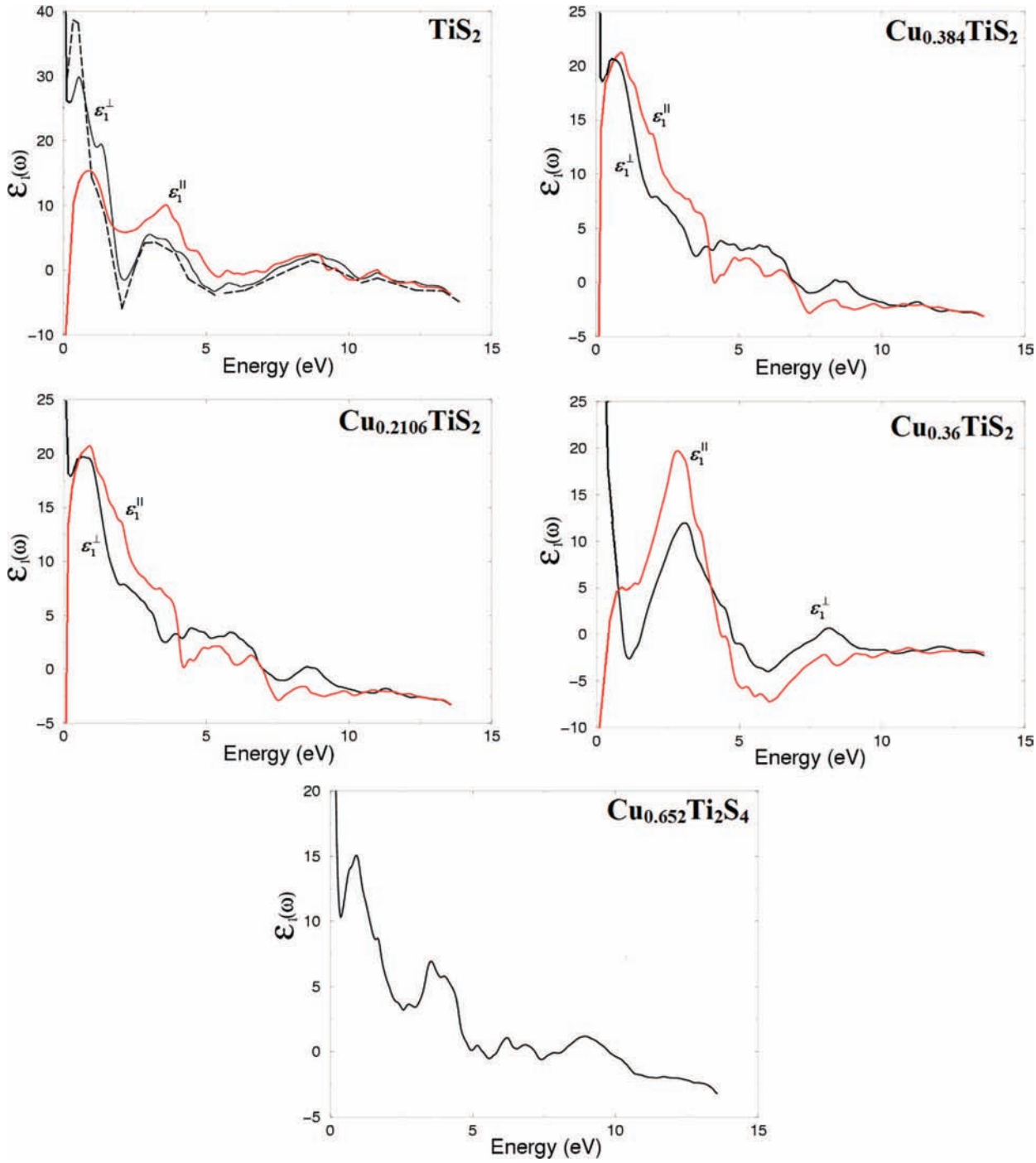

Figure 6. Calculated $\varepsilon_1(\omega)$, $\varepsilon_1^{\perp}(\omega)$ (dark curve), and $\varepsilon_1^{\mathrm{II}}(\omega)$ (light curve) for the host material TiS_2 and its intercalated compounds $Cu_{0.384}TiS_2$, $Cu_{0.2106}TiS_2$, $Cu_{0.36}TiS_2$, and $Cu_{0.652}Ti_2S_4$ in comparison with the available experimental data of $\vec{E} \perp c$[26] (dashed curve), for the host material TiS_2.

the structures above 5 eV in $\varepsilon_2^{||}(\omega)$ and $\varepsilon_2^{\perp}(\omega)$ are dominated by transitions from the top (and bottom) of occupied Cu-s/p/d, S-s/p, and Ti-s/p/d states to the top/bottom of unoccupied Cu-s/p/d, S-s/p, and Ti-s/p/d states. The real parts $\varepsilon_1(\omega)$, $\varepsilon_1^{||}(\omega)$, and $\varepsilon_1^{\perp}(\omega)$ are obtained using the Kramers−Kronig relations.[54]

$$\varepsilon_1(\omega) = 1 + \frac{2}{\pi} P \int_0^{\infty} \frac{\omega' \varepsilon_2(\omega')}{\omega'^2 - \omega^2} \, d\omega' \qquad (9)$$

where P implies the principal value of the integral.

Figure 6 shows $\varepsilon_1^{||}(\omega)$, $\varepsilon_1^{\perp}(\omega)$, and $\varepsilon_1(\omega)$ for the host and the Cu-intercalated compounds. The first structure around 1 eV shows the highest peak intensity in these spectra. The main peak is followed by small structures oscillated around the zero position, then takes on negative values at the high energies. At the low energy range, the effect of Drude term is considerable. The calculated $\varepsilon_1^{||}(\omega)$ and $\varepsilon_1^{\perp}(\omega)$ spectra are anisotropic. In the low energy range up to 5 eV, $\varepsilon_1^{||}(\omega)$ dominates; thereafter, both polarizations contribute. We compare our calculated dielectric functions with the available experimental data;[26] for $\vec{E} \perp c$, good agreement was found. This agreement is attributed to use of the full potential method, which has proven to be one of the most accurate methods[55,56] for the computation of the electronic structure of solids within DFT. It is necessary to emphasize that use of the full potential approach has substantial advantages

compared to the pseudopotential method,[57] which is not sensitive to the anisotropy in the layered crystalline structures.

We have made a detailed comparison with the host material and its experimental data to ascertain the effect of Cu intercalation on the optical properties. We find that the optical properties of Cu-intercalated compounds are significantly influenced by the location and the concentrations of the intercalated Cu atoms.

IV. Conclusion

The structural and optical properties for TiS_2 and its intercalated compounds with different sites and concentrations of Cu have been calculated using the full potential method. We demonstrate the effect of using a full potential method on the band structure, density of states (DOS), and the optical properties of intercalated compounds. We compare our results of Cu-intercalated compounds with the host TiS_2 to ascertain the effect of changing the sites and concentrations of the intercalated Cu on the electronic and optical properties. We notice that changing the sites and the concentrations of the intercalated Cu causes dramatic changes in the band structure, resulting in more bands cutting E_F. From the PDOS of the host compound, we note that there is a strong hybridization between S-p states and Ti-d states below E_F. This hybridization becomes weak in the intercalated compounds. In all compounds, Cu-s strongly hybridizes with Cu-p below and above E_F. Our calculated optical properties of the host material show reasonable agreement with the available experimental data. This agreement is attributed to our use of the full potential method, which has proven to be one of the most accurate methods for the computation of the electronic structure of solids within density functional theory.

The Cu-s and Cu-p bands are very broad and contribute much to the density of states. Our calculations show that the electronic and optical properties are influenced significantly by the location and the concentrations of the intercalated Cu in TiS_2.

Our calculated density of states and the electron charge density show that in the host and the intercalated compounds, all the Ti−Ti and S−S bonds are basically of ionic character, and Ti−S bonds are of covalent character. No covalent electrons are found between Cu and S atoms; that is, no covalent bond exists between the Cu and S atoms. The Cu atoms are ionic in the intercalated compounds.

Acknowledgment. This work was supported from the institutional research concept of the Institute of Physical Biology, UFB (No. MSM6007665808) and the Institute of System Biology and Ecology, ASCR (No. AVOZ60870520).

References and Notes

(1) (a) Whittingham, M. S. *Prog. Solid State Chem.* **1978**, *12*, 1. Thackeray, M. M.; Thomas, J. O.; Whittingham, M. S. *MRS Bull* **2000**, *25* (3), 39.
(2) Winter, M.; Besenhard, J. O.; Spahr, M. E.; Novak, P. *Adv. Mater.* **1998**, *10*, 725.
(3) Megahed, S.; Scrosati, B. *The Electrochem. Soc. Interface* **1995**, *4* (4), 34.
(4) Johnson, W. B.; Worrell, W. L. *Synth. Mater.* **1982**, *4*, 225–248.
(5) Basu, S.; Worrell, W. L. In *Fast Ion Transport in Solids*; Vashishta, P.; Mundy, J. N.; Shenoy, G. K., Eds.; Elsevier North Holland, Inc.: New York, 1979, 149−152.
(6) Wilson, J. A.; Yoffe, A. D. *Adv. Phys.* **1969**, *18*, 193.
(7) Umrigar, G.; Ellis, D. E.; Wang, D. S.; Krakauer, H.; Posternak, M. *Phys. Rev. B* **1982**, *26*, 4935.
(8) Greenway, D. L.; Nitsche, R. T. *Phys. Chem. Solids* **1965**, *26*, 1445.
(9) Beal, A. R.; Knights, J. C.; Liang, W. Y. *J. Phys. C* **1972**, *5*, 3540.
(10) Liang, W. Y.; Lucovsky, G.; White, R. M.; Stutius, W.; Pisharody, K. R. *Philos. Mag.* **1976**, 33493.
(11) Murray, R. B.; Yoffe, A. D. *J. Phys. C* **1972**, *5*, 3038.
(12) Klipstein, P. C.; Friend, R. H. *J. Phys. C* **1984**, *17*, 2713.
(13) Benesh, G. A.; Woolley, A. M.; Umrigar, C. *J. Phys. C* **1985**, *13*, 1595.
(14) Fang, C. M.; de Groot, R. A.; Hass, C. *Phys. Rev. B* **1997**, *56*, 4455.
(15) Wu, Z. Y.; Ouvrard, G.; Lemaux, S.; Moreau, P.; Gressier, P.; Lemoigno, F. *Phys. Rev. Lett.* **1996**, *77*, 210. Wu, Z. Y.; Lemoigno, F.; Gressier, P.; Ouvrard, G.; Moreau, P.; Rouxel, J.; Natoli, C. R. *Phys. Rev. B* **1996**, *54*, R11009.
(16) Wu, Z. Y.; Ouvrard, G.; Moreau, P.; Natoli, C. R. *Phys. Rev. B* **1997**, *55*, 9508.
(17) Allan, D. R.; Kelsey, A. A.; Clark, S. J.; Angel, R. J.; Ackland, G. J. *Phys. Rev. B* **1998**, *57*, 5106.
(18) Yang-Soo, K.; Masataka, M.; Isao, T.; Hirohiko, A. *Jpn. J. Appl. Phys* **1998**, *37*, 4878.
(19) Sharma, S.; Nautiyal, T.; Singh, G. S.; Auluck, S.; Ambrosch-Draxl, C. *Phys. Rev. B* **1999**, *59*, 14833.
(20) Bocharov, S.; Drager, G.; Heumann, D.; Simunek, A.; Sipr, O. *Phys. Rev. B* **1998**, *58*, 7668.
(21) Simunek, A.; Sipr, O.; Bocharov, S.; Heumann, D.; Drager, G. *Phys. Rev. B* **1997**, *56*, 12232.
(22) Fischer, D. W. *Phys. Rev. B* **1973**, *8*, 3576.
(23) Borghesi, A.; Chen-jia, C.; Guizzetti, G.; Nosenza, L.; Reguzzoni, E.; Stella, A.; Levy, F. *Phys. Rev. B* **1984**, *33*, 2422.
(24) Nagaosa, N.; Hanamura, E. *Phys. Rev. B* **1984**, *29*, 2060.
(25) Hughes, H. P.; Liang, W. Y. *J. Phys. C* **1977**, *10*, 1079.
(26) Bayliss, S. C.; Liang, W. Y. *J. Phys. C* **1982**, *15*, 1283.
(27) Bayliss, S. C.; Liang, W. Y. *J. Phys. C* **1985**, *18*, 3327.
(28) Borghesi, A.; Guizzetti, B.; Nosenzo, L.; Reguzzoni, E.; Stella, A. *Nuovo Cimento* **1984**, *4D* (2), 141.
(29) Baldassarre, L.; Levy, A. *Opt. Commun.* **1989**, *72*, 71 P.
(30) Reshak, A. H.; Auluck, S. *Phys. Rev. B* **2003**, *68*, 125101.
(31) Reshak, A. H. *Physica B* **2006)** , *373*, 1.
(32) Reshak, A. H.; Auluck, S. *Phys. Rev. B* **2003**, *68*, 245113.
(33) Reshak, A. H.; Kityk, I. V.; Auluck, S. *J. Chem. Phys.* **2008**, *129*, 074706.
(34) Reshak, A. H.; Auluck, S. *Phys. Rev. B* **2003**, *68*, 195107.
(35) Kusawake, T.; Takahashi, Y.; Wey, M. Y.; Ohshima, K. *J. Phys. C* **2001**, *13*, 9913.
(36) Kusawake, T.; Takahashi, Y.; Ohshima, K.; Wey, M. Y. *J. Phys. C* **1999**, *11*, 6121.
(37) Kusawake, T.; Takahashi, Y.; Ohshima, K. *Mater. Res. Bull.* **1998**, *33*, 1009.
(38) Kuwabara, K.; Sugiyama, K. *J. Appl. Electrochem.* **1986**, *16*, 23.
(39) Kanno, R.; Takeda, Y.; Imura, M.; Yamamoto, O. *J. Appl. Electrochem.* **1982**, *12*, 681.
(40) Degenhakdt, D.; Rabe, P.; Haense, R. *Physica Status Solidi, A* **2006**, *95*, 439.
(41) Julien, C.; Samaras, I.; Gorochov, O.; Ghorayed, A. M. *Phys. Rev. B* **1992**, *45*, 13390.
(42) Blaha, P.; Schwarz, K.; Madsen, G. K. H.; Kvasnicka, D.; Luitz, J. *WIEN2K, An Augmented Plane Wave + Local Orbitals Program for Calculating Crystal Properties*; Karlheinz Schwarz, Techn. Universitat: Wien, Austria, 2001, ISBN 3-9501031-1-2.
(43) Hohenberg, P.; Kohn, W. *Phys. Rev. B* **1964**, *136*, 864.
(44) Perdew, J. P.; Burke, S.; Ernzerhof, M. *Phys. Rev. Lett.* **1996**, *77*, 3865.
(45) Jepsen, O.; Andersen, O. K. *Solid State Commun.* **1971**, *9*, 1763. (a) Lehmann, G.; Taut, M. *Phys. Status Solidi B* **1972**, *54*, 496.
(46) Wilson, J. A.; Yoffe, A. D. *Adv. Phys.* **1969**, *18*, 193.
(47) Takahira, Y.; Noshi, S.; Kazuko, M. *J. Phys. C* **1987**, 20.
(48) Yang-Soo, K.; Masataka, M.; Isao, T.; Hirohiko, A. *Jpn. J. Appl. Phys.* **1998**, *37*, 4878.
(49) Ohshima, K.; Moss, S. C. *Acta Crystallogr., A* **1983**, *39*, 298.
(50) Kuroiwa, Y.; Ohshima, K.; Watanabe, Y. *Phys. Rev. B* **1990**, *42*, 11591.
(51) Wiegers, G. A.; Bouwmeester, H. J.; Gerards, A. G. *Solid State Ionics* **1985**, *16*, 155.
(52) Khan, M. A.; Kashyap, A.; Solanki, A. K.; Nautiyal, T.; Auluck, S. *Phys. Rev. B* **1993**, *23*, 16974.
(53) Hufner, S.; Claessen, R.; Reinert, F.; Straub, Th.; Strocov, V. N.; Steiner, P. *J. Electron Spectra Relat. Phenom.* **1999**, *100*, 191.
(54) Wooten, F., *Optical Properties of Solids*; Academic Press: New York, London, 1972.
(55) Shiwu, G. *Comput. Phys. Commun.* **2003**, *153*, 190–198.
(56) Schwarz, K. *J. Solid State Chem.* **2003**, *176*, 319–328.
(57) Kolinko, M. I.; Kityk, I. V.; Krochuk, A. S. *J. Phys. Chem.* **1992**, *53*, 1315–1320; *J. Phys. Chem. Solids* **53**, *1315*, 1992.

JP810242W